

# SPECKLE INTERFEROMETRY OF SECONDARY COMPONENTS IN NEARBY VISUAL BINARIES<sup>†</sup>

ANDREI TOKOVININ

Cerro Tololo Inter-American Observatory, Casilla 603, La Serena, Chile

ELLIOTT P. HORCH

Department of Physics, Southern Connecticut State University, 501 Crescent Street, New Haven, CT 06515, USA

*Draft version September 4, 2020*

## ABSTRACT

Statistical characterization of secondary subsystems in binaries helps to distinguish between various scenarios of multiple-star formation. The DSSI speckle instrument was used at the Gemini-N telescope for several hours in 2015 July to probe binarity of 25 secondary components in nearby solar-type binaries. Six new subsystems were resolved, with meaningful detection limits for the remaining targets. The large incidence of secondary subsystems agrees with other similar studies. The newly resolved subsystem HIP 115417 Ba,Bb causes deviations in the observed motion of the outer binary from which an astrometric orbit of Ba,Bb with a period of 117 years is deduced.

*Subject headings:* binaries: visual; stars: low-mass

## 1. INTRODUCTION

Formation of multiple systems is an active research topic related to such areas as stellar mass function, disks, and initial conditions for planet formation. Although large-scale numerical simulations give reasonable match to the observed statistics (Bate 2012), we are still far from modeling the distributions of multiple-star parameters in a predictive way. The relevant physics is identified, but the correct mix of processes that define multiple-star population is yet to be found.

Stochastic dynamics of small  $N$ -body systems is one such process. Recently Reipurth & Mikkola (2012) suggested that wide binaries are mostly formed by ejections from smaller  $N$ -body aggregates. It is well known that in chaotic dynamics the smallest-mass stars are ejected most readily. We therefore would expect wide companions to be preferentially of low mass, single, and on eccentric orbits. Another physical process – rotationally-driven fragmentation – makes the opposite prediction (Delgado-Donate et al. 2004). In this case, wide binaries contain a large fraction of the collapsing cloud’s angular momentum. Their orbits should have moderate eccentricity, the masses of both wide components should be comparable, and the incidence of subsystems in the primary and secondary components should be similar.

In this paper we focus on multiplicity of secondary components of wide binaries, so far poorly characterized. The primary components of those binaries are nearby solar-type dwarfs; their multiplicity is constrained by combination of methods, from radial velocities (RVs) for close pairs to imaging and wide common-proper-motion (CPM) binaries, spanning the full range of periods (Tokovinin 2014a). In contrast, the fraction of subsystems in the secondary components could be estimated with a considerable uncertainty. Yet, this is an important diagnostic of the formation processes. If secondary components were ejected on their wide orbits by dynam-

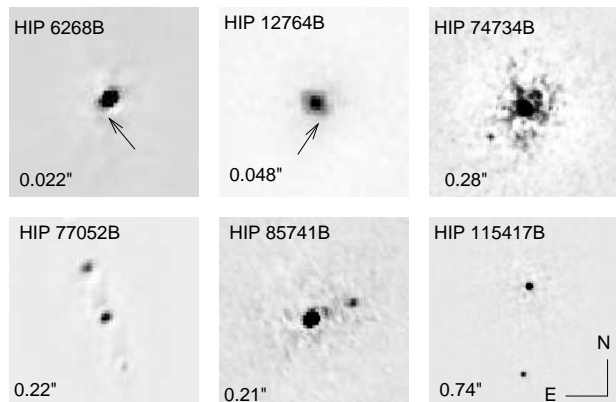


FIG. 1.— Negative images of newly resolved subsystems at 880 nm. The scale and intensity stretch are adjusted individually to highlight the companions. The numbers in the lower left corner of each image are angular separations. The first two resolutions (HIP 6268B and HIP 12764B) are tentative.

ical interplay in compact and unstable nascent multiple systems, they should be preferentially single.

In recent years, the binarity of secondary components has been probed by several techniques. Adaptive optics (AO) imaging was used at Gemini-S (Tokovinin et al. 2010), Palomar 1.5-m Robo-AO (Law et al. 2010; Riddle et al. 2015), and SOAR (Tokovinin 2014b); RVs were monitored by Tokovinin (2015). This project explores the binarity of secondary components by means of speckle interferometry at the 8-m Gemini-N telescope. Compared to the Robo-AO, a 7-fold increase in the angular resolution gives access to much shorter periods, exploring a larger part of the parameter space and overlapping with the RV surveys.

In Section 2 we describe the instrument, observations, and data reduction. Newly resolved binaries and detection limits are presented in Section 3. In Section 4 we analyze one of the newly discovered subsystems and determine its orbit using archival measurements of the wide outer binary. Section 5 concludes the paper.

## 2. OBSERVATIONS AND DATA REDUCTION

atokovinin@ctio.noao.edu  
horche2@southernct.edu

<sup>†</sup> Based on observations obtained at Gemini-N.

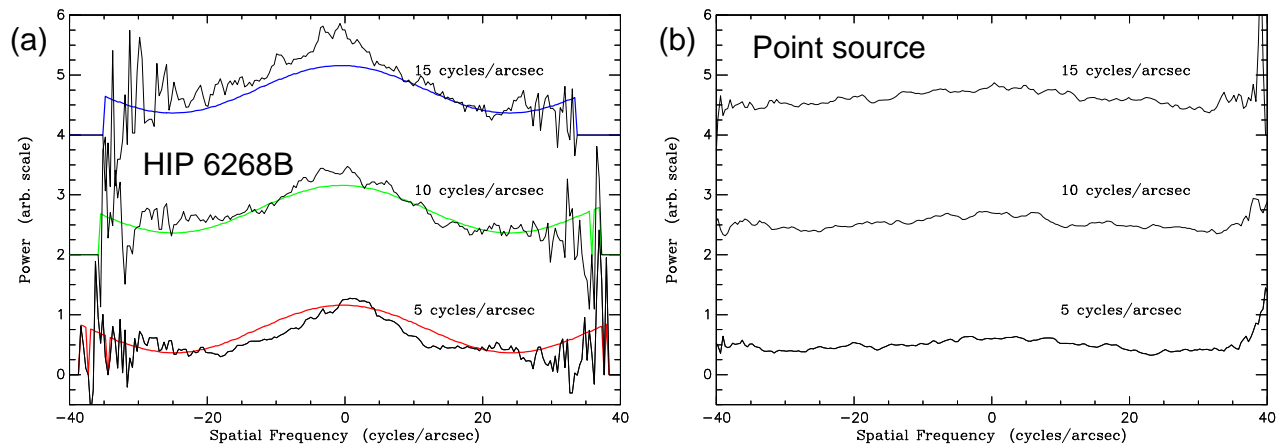


FIG. 2.— Left panel (a): cuts in the final fitted power spectrum perpendicular to the fringe direction for the marginal detection of HIP 6268 Ba,Bb at 880 nm. Three cuts are shown, each of which has a closest approach to the origin of the uv plane of 5, 10, and 15 cycles per arcsecond as shown (i.e. this value is measured parallel to the fringe direction). The fitted binary model is plotted with the colored curves. A similar analysis for a point source, where no fit is presented, is shown in the right panel (b). This gives a sense of how flat a typical point source observation is in the frequency domain and how significant the binary signal is.

Observing time for this work has been granted through NOAO (program 15A-0087) for a total of 7 hours, with a low Band 3 priority. This project was a “filler” for more challenging observations, as it could be executed in less than optimum conditions. The observations at Gemini-N were conducted by E.H., Mark Everett (NOAO), Steve Howell (NASA-Ames), Johanna Teske (DTM and Carnegie Observatories), and Lea Hirsch (UC Berkeley), between 2015 July 11 and 19. During this run, the sky was clear for about 2/3 of the time, allowing to use 4.7 hours for this program, part of it through the clouds.

The target list was based on the 67-pc sample of solar-type stars (Tokovinin 2014a). Known binaries with separations from  $0''.5$  to  $2''.8$  that had no prior high-resolution data from AO or speckle instruments were selected. Such binaries fit in the camera field of view, allowing to check both components for the existence of close subsystems. In addition, secondary components of wider binaries with separations from  $3''$  to  $10''$  were targeted separately. The program contained 63 targets; for 39 of those useful data could be obtained. In some cases, the brighter component A was pointed instead of the intended secondary B, either by error or because the extinction was too great to successfully observe the secondary while the primary was still visible.

The Differential Speckle Survey Instrument, DSSI, is described by Horch et al. (2009). Speckle images of the observed star are recorded by two electron multiplication CCDs simultaneously in two spectral bands, the light being divided by a dichroic. At Gemini-N, the DSSI worked with the filters that transmit central wavelengths and bandwidths of 692/40 and 880/50 nm; for brevity they are called here bands *R* and *I*. Previous publications resulting from the DSSI at Gemini-N, e.g. (Horch et al. 2012, 2015a), contain additional details. In a typical observing sequence, 1000 frames with a 60-ms exposure and a  $256 \times 256$  size are recorded in both DSSI channels simultaneously. Observations of single unresolved reference stars are taken at low airmass and used for modeling instrument signatures and atmospheric dispersion during data reduction. The data cubes are processed by the standard speckle technique (calculation of power spectrum and autocorrelation) and by the speckle image

reconstruction delivering true images (see further details in Horch et al. 2009, 2015b). Figure 2 illustrates the resolution of a very close binary HIP 6268B.

The pixel scale of 11.41 mas and the orientation of both detectors was calibrated as described by Horch et al. (2012). We observed two binaries, HIP 83838 = HU 1176 and HIP 104858 = STT 535, for which extremely accurate interferometric orbits are available (Muterspaugh et al. 2008, 2010). After correcting the optical distortion in the reflective channel of the DSSI (Horch et al. 2011), we found astrometry in the two channels to be in excellent mutual agreement at a level of  $\sim 2$  mas for most pairs, in line with the previous analysis of Gemini-N speckle data in (Horch et al. 2012); larger discrepancies are present only for pairs near the limit of the technique.

Although the detectors used with DSSI have a  $512 \times 512$  pixel format, the speckle frames were sub-arrays of  $256 \times 256$  pixels centered on the target, so the field of view of the recorded images was  $2''.8 \times 2''.8$ . This allows detection of companions with separations up to  $1''.45$ . Some wider binaries (up to about  $2''$  separation) were measured by placing both components in the field, i.e. centering the sub-array in between the two sources.

### 3. RESULTS

#### 3.1. Measurements

Binary companions, either known or newly discovered, were identified visually in the reconstructed images (Figure 1). Relative astrometry and photometry of binary stars is derived by approximating the speckle power spectrum, as described in the previous DSSI publications (Horch et al. 2009, 2012). The detection limits are estimated by computing rms fluctuations  $\sigma$  in annular zones of the reconstructed image and assuming that a companion above  $5\sigma$  would be detectable, see (Horch et al. 2011). Figure 3 illustrates the detection limits in the *I* channel.

High contrast ( $\Delta m$  of 4 to 6 mag) and high-SNR DSSI observations at Gemini, such as those described here, generally detect companions down to a separation of about  $0''.1$ . For smaller separations, the dynamic range decreases to something below  $\Delta m \sim 1$  mag at the diffrac-

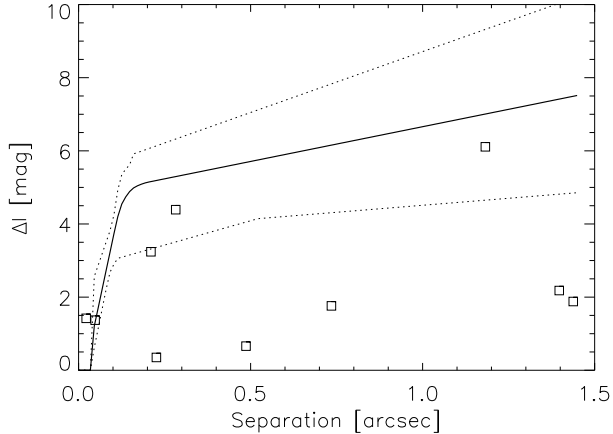


FIG. 3.— Detection limits in the  $I$  channel of DSSI. The full line is the average detection curve, the dotted lines are the best and worst detection limits. Squares denote the actually measured binaries.

TABLE 2  
RESIDUALS TO ORBITS

HIP	$(O-C)_\theta$ ( $^\circ$ )	$(O-C)_\rho$ ( $''$ )	Gr.	Reference
9621	-3.7	-0.105	3	Heintz (1996)
82510	-0.5	0.048	3	Scardia et al. (2003)
95589	0.0	0.023	4	Scardia et al. (2015)
97477	-0.1	0.000	2	Mason et al. (2006)

tion limit. We have looked for evidence of vibration effects in our data by studying the centroid positions of bright stars as a function of time, but have not found any signature of vibration to the limit of our time resolution, which is about 20 Hz. Elongations in speckles do occur, but these are correlated with telescope elevation and directed along a line leading to the zenith as DSSI does not correct the atmospheric dispersion. This we have calibrated out by deconvolving our data with point source observations that have a dispersion model built in (the elongation is measured on a bright star observed at small zenith distance  $z$  and scaled as  $\tan z$  when deconvolving the object). The resulting reconstructed images remain diffraction limited.

Table 1 lists all observations. Its first column identifies the target by the *Hipparcos* number of the primary component, while the next column shows which component was observed, the primary A or the secondary B; AB stands for both components. The following columns contain the Besselian date of the observation, filter ( $R$  or  $I$ , see above), and the detection limits  $\Delta m$  at separations of  $0''.15$  and  $1''$ . For resolved binaries, the last three columns give the position angle  $\theta$ , separation  $\rho$ , and magnitude difference  $\Delta m$ , while the detection limits for resolved binaries are  $\Delta m$  relative to the primary component.

Four binaries have known orbits. Residuals from our measurements (average in  $R$  and  $I$  filters) to those orbits are given in Table 2, as a consistency check of the DSSI calibration. However, they are much larger than the DSSI errors of  $\sim 1$  mas (Horch et al. 2012) and reflect the quality of the orbits. The 4th column gives the orbit grade from (Hartkopf, Mason & Worley 2001).

### 3.2. Comments on individual systems

Comments on some observed objects are given here. Orbital periods of newly resolved pairs are estimated by assuming that projected separation equals semimajor axis. Overall, we resolved six new subsystems in the secondary components. One of them was independently found by other team. The two closest subsystems are tentative and require confirming observations.

*HIP 6268.* The faint secondary component of this binary was pointed and tentatively resolved into a new 20-mas pair Ba,Bb. The  $2''.6$  separation between A and B was last measured in 1967; presently AB must be wider than  $2''.8$ , as it did not fit into the DSSI field. The separation of Ba,Bb implies a period of 1.3 yr. Given the small separation, the relative photometry  $\Delta R = 1.08$  mag and  $\Delta I = 1.42$  mag is not reliable and it is premature to conclude that Bb is bluer than Ba. The masses of Ba and Bb estimated from their luminosity are 0.6 and  $0.4 M_\odot$ . Ironically, the main component A has never been observed with high angular resolution and has no RV coverage, so a similarly close subsystem Aa,Ab would remain undetected, if it existed.

*HIP 9583.* Both A and B were observed separately, the separation of AB is  $2''.3$ . The data quality is below average because light from the other component is getting into the speckle frames of the observed component. This gives a “bright” edge to these frames, and it is not handled well by the reduction routines, causing lines in the reconstructed images. But nonetheless, the power spectra show no hint of any fringes, so there is no evidence for binarity for either component.

*HIP 12764.* The secondary component B of the recently discovered  $5''.1$  binary was observed and resolved into a  $0''.048$  subsystem Ba,Bb. However, the pair is not seen in the  $R$ -band, and this detection remains tentative. Both A and B were also observed with the speckle camera at SOAR and unresolved (Tokovinin et al. 2016). The period of Ba,Bb is estimated at 2.6 yr, the masses are 0.7 and  $0.5 M_\odot$ . The main component A has an RV trend (Bonavita & Desidera 2007) also indicative of a subsystem. Therefore, the DSSI data reveal this as a potential new 2+2 quadruple system.

*HIP 12925.* This is a quadruple system where the main star A is a spectroscopic binary with yet unknown orbit and two visual companions. The components A and D, at  $1''.9$  separation, were pointed separately and found unresolved. The pair AD was also observed at Palomar in 2013 (Roberts et al. 2015), with no new subsystems detected either.

*HIP 74211.* The B-component of STF 1916 was unresolved. It contains a spectroscopic subsystem (D. Latham, 2012, private communication).

*HIP 74734.* The secondary component of the  $5''.4$  pair HO 547 is resolved into a new subsystem Ba,Bb with a relatively wide separation of  $0''.28$  but a high contrast. It is barely seen in the  $R$  channel, and its tentative measure in  $R$  disagrees with the reliable measure in  $I$ . We estimate the period of Ba,Bb as 50 yr, the masses are 0.65 and  $0.12 M_\odot$ . This resolution highlights the high dynamic range of DSSI.

*HIP 77052.* Both components of the  $4''.4$  nearby (parallax 68 mas) pair A 2230 ( $\psi$  Ser, GJ 596.1) were observed, and Ba,Bb was resolved at  $0''.22$ . This subsystem

has been independently discovered by Rodriguez et al. (2015). We estimate the masses of nearly equal stars Ba and Bb as  $0.25 M_{\odot}$ . The position of Ba,Bb in 2009.5 was  $(31^{\circ}, 0''.22)$ , similar to  $(27^{\circ}, 0''.22)$  in 2015.5, so the pair may have already completed a full revolution. It was measured again at SOAR on 2016.141 at  $(21^{\circ}.8, 0''.202)$ , demonstrating fast retrograde motion. The three measures correspond to a 6.1-year orbit with a semimajor axis of  $0''.19$  and a mass sum of  $0.5 M_{\odot}$ , but it is premature to present this tentative orbit here. Masses of Ba and Bb will eventually be measured accurately from the orbit to test evolutionary models of late M-dwarfs, while the main component A, a G5V solar analogue with a constant RV, will serve as a reference. The 529-year orbit of the outer binary AB recently determined by Gatewood & Mason (2013) corresponds to the mass sum of  $1.44 M_{\odot}$ , in agreement with the estimated masses of all three stars.

*HIP 81662*. Both A and B at  $11''.6$  from each other were pointed separately and found unresolved. A trend in the RV of A has been noted by Bonavita & Desidera (2007).

*HIP 85741*. The secondary component of the  $5''.3$  pair HU 673 is resolved at  $0''.2$ , with a large  $\Delta m$ . The period of Ba,Bb is  $\sim 50$ yr, masses  $0.55$  and  $0.14 M_{\odot}$ .

*HIP 100970* hosts a planet with 18-day orbit (Fischer et al. 1999) and has a faint visual companion B at  $3''.5$ . We report a secure non-resolution of the main star, in agreement with other publications, while B has not been observed.

*HIP 101345* is the pair BU 668 with a large contrast, last measured at  $3''.2$  in 1965 and now found at  $1''.2$ . It has not been resolved by *Hipparcos*.

*HIP 110785* is a triple system consisting of the 913-day spectroscopic and astrometric binary Aa,Ab (Griffin 2010) in a  $3''.6$  binary BU 290 with a poorly constrained visual orbit. The estimated masses of Aa and Ab are  $1.5$  and  $0.3 M_{\odot}$ , the semi-major axis of Aa,Ab is  $59$ mas. The subsystem Aa,Ab is unresolved here; its highly inclined orbit means that the separation can often be smaller than the semimajor axis.

*HIP 111903* is a  $10''.9$  pair HU 3128 where a spectroscopic subsystem in the primary component A is suspected from RV variation (Tokovinin 2015). The secondary component B is unresolved here.

*HIP 115417* has a newly resolved secondary subsystem, discussed in the next Section. There was some confusion about which component, A or B, was pointed at Gemini and resolved. Analysis of the astrometric data indicates that the subsystem belongs to B. This was confirmed in 2015 September using speckle camera at the SOAR telescope (Tokovinin et al. 2016). The SOAR measure of Ba,Bb (2015.7379:  $181^{\circ}.2, 0''.746, \Delta m = 1.97$  mag at  $788$ nm) agrees very well with the Gemini measure (2015.5255:  $180^{\circ}.6, 0''.735, \Delta I = 1.76$  mag).

#### 4. THE TRIPLE SYSTEM HIP 115417

HIP 115417 (HD 220334, WDS 23228+2034) is a nearby solar-type binary with the following properties: spectral type G2V, HIP2 parallax  $26.75 \pm 0.62$  mas, proper motion  $(+314.6, -11.7)$  mas yr $^{-1}$  (van Leeuwen 2007),  $V = 6.62$  mag. The WDS database contains 262 measurements of AB. The pair was frequently observed photographically from 1942 to 1976 (mostly at USNO),

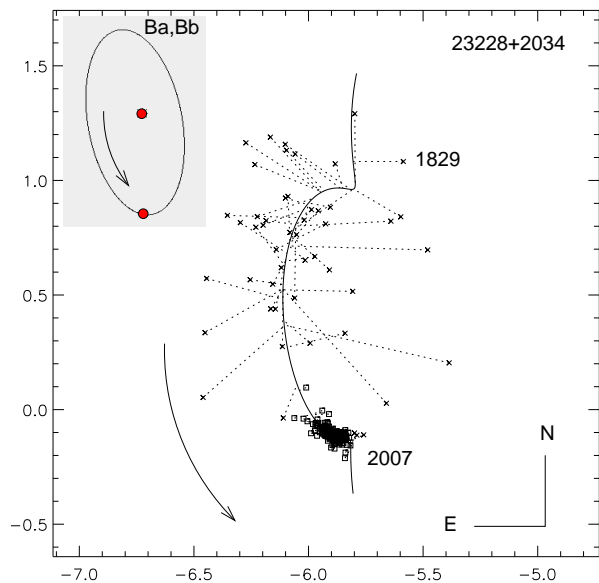


FIG. 4.— Motion of the component B relative to A, located at coordinate origin, in the binary system HIP 115417 (STF 3007). Visual observations are plotted as crosses, photographic observations as squares. The line shows the trajectory corresponding to the two orbits proposed here. The scale is in arcseconds. The gray insert shows the orbit of Ba,Bb and the observed position of this pair on different scale.

probably in search of astrometric subsystems.

The visual binary AB was discovered by W. Struve in 1829 at  $5''.69$  and  $79^{\circ}.5$  (STF 3007). It has moved to  $5''.85$  and  $92^{\circ}.1$  in 2007. Estimated period of this pair is on the order of 2kyr. The Tycho photometry gives  $V$  magnitudes of 6.74 and 9.78 mag,  $B$  magnitudes of 7.42 and 10.98 mag for A and B, respectively. The distant visual companion C, also discovered by Struve, is optical.

The motion of AB observed for nearly two centuries shows a “wavy” character, most obvious in the position angles and less evident in separations, which are measured less accurately than angles. The astrometric subsystem Ba,Bb responsible for this wave was first resolved by us and confirmed at SOAR two months later. Archival observations of AB allow us to estimate orbital parameters of the subsystem.

If the orbit of the subsystem Ba,Bb is eccentric, the center of mass does not coincide with the center of the orbital ellipse. When we subtract the smooth motion of AB, this offset is also subtracted and the average residuals are zero; an astrometric orbit derived from such residuals would have a small eccentricity, even if  $e$  is in fact substantial. This problem is solved by fitting the motion of AB and the orbit of the subsystem Ba,Bb simultaneously. We represent the motion of AB by a circular orbit and adjust its parameters to obtain the expected mass sum. Obviously, the orbit of AB is premature, it is derived here only to model its observed segment, as needed for the analysis of the subsystem. The astrometric orbit of B (photo-center of the subsystem Ba,Bb) is described by the standard seven Campbell elements ( $P$ – period,  $T_0$  – time of periastron,  $e$  – eccentricity,  $a$  – astrometric semimajor axis,  $\Omega$  – position angle of node,  $\omega$  – argument of periastron,  $i$  – inclination). An additional parameter  $F = A_2/a_2$ , the ratio of the true and astrometric inner

TABLE 3  
ORBITS OF HIP 115417

Element	AB	Ba,Bb
$P$ (yr)	2161	117 (fixed)
$T_0$ (yr)	1904.5	$1935.1 \pm 5.5$
$e$	0 (fixed)	$0.204 \pm 0.04$
$a$ (")	6.053	$0.215 \pm 0.011$
$\Omega$ ( $^\circ$ )	84.4	$188.5 \pm 2.8$
$\omega$ ( $^\circ$ )	0 (fixed)	$294 \pm 15$
$i$ ( $^\circ$ )	58 (fixed)	$65.1 \pm 2.5$
$F = A_2/a_2$	...	$3.21 \pm 0.17$

axes, is introduced, and the resolved measures of Ba,Bb are added to the data set. Thus, the data are modeled by 15 parameters.

The early visual measurements of AB are inaccurate and are compatible with a wide range of orbital parameters, while the photographic measurements do not cover the full inner period. To derive the most likely set of orbital elements, we estimate the components' masses from their luminosity using standard relations for main sequence stars and choose the elements that match those masses, namely 1.2, 0.8, and  $0.5 M_\odot$  for A, Ba, and Bb, respectively. This is achieved by fixing some elements in the least-squares fitting. By increasing the inclination of the outer circular orbit, we increase the total mass sum. The inner mass sum is adjusted by fixing the inner period. The number of adjustable parameters is therefore reduced from 15 to 11.

In the least-squares adjustment of 11 free parameters, the weights are inversely proportional to the measurement errors, which are assigned subjectively based on the observing method and then corrected iteratively to down-weight the outliers. The errors of most micrometer measures are taken as  $0''.2$ , the errors of photographic measures are  $0''.02$ , in both radial and tangential directions. The weighted rms deviation from the orbits is indeed 20 mas. Figure 4 shows the measures of AB and the trajectory corresponding to the elements listed in Table 3.

If the light of the component Bb is negligible, the measures of AB and A,Ba are identical and the mass ratio in the inner subsystem is related to the ratio of the axes,  $q_2 = 1/(F - 1) = 0.45$  for  $F = 3.2$ . The estimated masses correspond to  $q_2 \approx 0.6$  or  $F \approx 2.7$ . The light of

Bb is thus slightly offsetting the photo-center of B from the position of Ba, increasing  $F$ . This semi-qualitative analysis is all we can do at present, as the data do not constrain both orbits sufficiently well to warrant a more detailed investigation. The long inner period means that the situation will not improve soon.

## 5. SUMMARY

We observed 25 secondary components of nearby binaries with the DSSI instrument and discovered six new subsystems (one of those was independently found by others). Two new pairs are very tight and have short estimated periods, illustrating the detection power of speckle interferometry at a 8-m telescope. The large fraction of resolved secondaries, 0.24, supports previous results (Tokovinin 2014b; Riddle et al. 2015; Tokovinin 2015) and shows that secondary subsystems are no less frequent than subsystems in the primaries. Considering the small number of targets covered, it makes little sense to go beyond this qualitative statement in the statistical analysis. The data collected here, including non-resolutions with deep detection limits, will be used in the future to obtain a refined statistical analysis of the complete 67-pc sample. The large incidence of secondary subsystems suggests that dynamical interactions in small  $N$ -body systems do not play a major role in the formation of multiple stars.

One of the newly resolved secondary subsystems, HIP 115417 Ba,Bb, causes noticeable deviation from the slow motion of the outer pair AB. We determined a preliminary orbit of the inner subsystem with a period of 117 years using archival measurements from the WDS.

We thank all observers who participated in the DSSI run. We are grateful to Gemini staff who aided in making the DSSI observations possible. This work used the SIMBAD service operated by Centre des Données Stellaires (Strasbourg, France), bibliographic references from the Astrophysics Data System maintained by SAO/NASA, and the Washington Double Star Catalog maintained at USNO.

*Facilities:* Gemini-N.

## REFERENCES

- Bate, M. 2012, MNRAS, 419, 3115  
 Bonavita, M. & Desidera, S. 2007, A&A, 468, 721  
 Delgado-Donate, E. J., Clarke, C. J., & Bate, M. 2004, MNRAS, 351, 617  
 Fischer, D. A., Marcy, G. W., Butler, P. et al. 1999, PASP, 111, 50  
 Gatewood, G. & Mason, B. D. 2013, IAUDS, 181, 1  
 Griffin, R. F. 2010, Obs, 1214  
 Hartkopf, W. I., Mason, B. D. & Worley, C. E. 2001, AJ, 122, 3472 (VB6)  
 Heintz, W. D. 1996, ApJS, 105, 475  
 Horch, E., van Altena, W. F., Cyr, W. M. et al. 2008, AJ, 136, 312  
 Horch, E. P., Veillette, D. R., Baena G. et al. 2009, AJ, 137, 505  
 Horch, E. P., Gomez, S. C., Sherry, W. H. et al. 2011, AJ, 141, 45  
 Horch, E. P., Howell, S. B., Everett, M. E. & Ciardi, D. R. 2012, AJ, 144, 165  
 Horch, E. P., van Altena, W. F., Demarque, P. et al. 2015a, AJ, 149, 151  
 Horch, E. P., van Belle, G. T., Davidson, J. W., Jr. et al. 2015b, AJ, 150, 151  
 Law, N. M., Dhital, S., Kraus, A. et al. 2010, ApJ, 720, 1727  
 Mason, B. D., Hartkopf, W. I., Wycoff, G. L., & Holdenried, E. R. 2006, AJ, 132, 2219  
 Muterspaugh, M. W., Lane, B. F., Fekel, F. C. et al. 2008, AJ, 135, 766  
 Muterspaugh, M. W., Hartkopf, W. I., Lane, B. F. et al. 2010, AJ, 140, 1623  
 Reipurth, B. & Mikkola, S. 2012, Nature, 492, 221  
 Riddle, R. L., Tokovinin, A., Mason, B. D. et al. 2015, ApJ, 799, 4  
 Roberts, L.C. Jr., Tokovinin, A., Mason, B.D. et al. 2015, AJ, 150, 130  
 Rodriguez, D. R., Duchêne, G., Tom, H. et al. 2015, MNRAS, 449, 3160  
 Scardia, M., Prieur, J.-L., Koechlin, L., & Aristidi, E. 2003, IAUDS, 149, 1  
 Scardia, M., Prieur, J.-L., Pansecchi, L. et al. 2015, IAUDS, 185, 1  
 Tokovinin A., Hartung M., & Hayward Th. L. 2010, AJ, 140, 510

Tokovinin, A. 2014a, AJ, 147, 86  
 Tokovinin, A. 2014b, AJ, 148, 72  
 Tokovinin, A. 2015, AJ, 150, 177

Tokovinin, A., Mason, B. D., Hartkopf, W. I. et al. 2016, AJ, 151,  
 153  
 van Leeuwen, F. 2007, A&A, 474, 653 (HIP2)

TABLE 1  
 SUMMARY OF RESULTS

HIP	Comp.	Date (+2000)	Filt.	$\Delta m(0.15)$ (mag)	$\Delta m(1)$ (mag)	$\theta$ ( $^{\circ}$ )	$\rho$ ( $''$ )	$\Delta m$ (mag)
3203	B	15.5475	R	5.6	7.1	...	...	...
3203	B	15.5475	I	5.3	7.8	...	...	...
6268	B	15.5338	R	5.6	7.1	125.6	0.019	1.08
6268	B	15.5338	I	5.6	7.1	124.8	0.022	1.42
9583	A	15.5393	R	3.9	4.9	...	...	...
9583	A	15.5393	I	4.3	5.3	...	...	...
9583	B	15.5393	R	3.7	5.4	...	...	...
9583	B	15.5393	I	3.2	5.4	...	...	...
9621	AB	15.5338	R	5.5	7.5	343.2	1.398	2.30
9621	AB	15.5338	I	5.6	7.2	343.2	1.397	2.18
12764	B	15.5366	R	4.6	4.8	...	...	...
12764	B	15.5366	I	4.8	5.2	237.2	0.048	1.37
12925	A	15.5365	R	5.6	6.9	...	...	...
12925	A	15.5365	I	5.3	7.5	...	...	...
12925	D	15.5365	R	3.0	4.0	...	...	...
12925	D	15.5365	I	4.9	5.9	...	...	...
74211	B	15.5248	R	5.5	6.7	...	...	...
74211	B	15.5248	I	5.5	6.7	...	...	...
74734	B	15.5248	R	5.3	6.7	133.3	0.286	7.14
74734	B	15.5248	I	5.4	7.2	130.2	0.282	4.39
74771	A	15.5300	R	5.8	8.1	...	...	...
74771	A	15.5300	I	5.9	7.1	...	...	...
77052	A	15.5248	R	4.1	5.9	...	...	...
77052	A	15.5248	I	4.1	5.6	...	...	...
77052	B	15.5409	R	4.8	6.0	27.0	0.227	0.28
77052	B	15.5409	I	4.8	5.6	26.9	0.226	0.35
78217	A	15.5329	R	4.4	6.9	...	...	...
78217	A	15.5329	I	5.4	7.2	...	...	...
78217	B	15.5355	R	4.4	5.5	...	...	...
78217	B	15.5355	I	4.9	6.4	...	...	...
79169	B	15.5355	R	4.6	4.8	...	...	...
79169	B	15.5355	I	5.1	6.0	...	...	...
80467	B	15.5329	R	4.6	4.8	...	...	...
80467	B	15.5329	I	4.7	5.0	...	...	...
81662	A	15.5301	R	5.7	8.7	...	...	...
81662	A	15.5301	I	5.6	8.3	...	...	...
81662	B	15.5437	R	4.9	5.7	...	...	...
81662	B	15.5437	I	4.6	6.7	...	...	...
82510	AB	15.5330	R	5.5	6.9	104.6	1.443	1.95
82510	AB	15.5330	I	5.5	6.6	104.9	1.438	1.88
82886	B	15.5329	R	4.5	4.9	...	...	...
82886	B	15.5329	I	4.9	5.5	...	...	...
85307	B	15.5437	R	4.7	5.0	...	...	...
85307	B	15.5437	I	5.1	6.0	...	...	...
85741	B	15.5464	R	4.7	5.2	292.4	0.207	4.16
85741	B	15.5464	I	5.2	6.1	293.8	0.210	3.24
95589	AB	15.5250	R	3.6	5.0	289.3	2.195	1.02
95589	AB	15.5250	I	4.2	5.2	289.7	2.186	0.82
97477	AB	15.5251	R	4.8	6.9	110.2	0.488	0.50
97477	AB	15.5251	I	4.8	6.9	110.5	0.487	0.66
98677	A	15.5251	R	4.3	7.4	...	...	...
98677	A	15.5251	I	4.5	7.6	...	...	...
99367	B	15.5251	R	5.4	7.5	...	...	...
99367	B	15.5251	I	5.2	7.5	...	...	...
100970	A	15.5251	R	5.3	8.3	...	...	...
100970	A	15.5251	I	5.2	8.0	...	...	...
101345	AB	15.5251	R	4.9	7.5	47.5	1.206	5.70
101345	AB	15.5251	I	4.8	7.9	47.8	1.182	6.11
104735	A	15.5281	R	5.7	9.3	...	...	...
104735	A	15.5281	I	5.9	8.7	...	...	...
107107	A	15.5281	R	5.5	8.9	...	...	...
107107	A	15.5281	I	5.9	8.3	...	...	...
110785	A	15.5253	R	4.2	6.8	...	...	...
110785	A	15.5253	I	4.7	5.9	...	...	...
111903	B	15.5281	R	4.9	5.5	...	...	...
111903	B	15.5281	I	5.7	7.1	...	...	...
112447	A	15.5255	R	4.9	6.2	...	...	...
112447	A	15.5255	I	4.8	6.7	...	...	...
113133	B	15.5281	R	5.7	7.8	...	...	...

TABLE 1 — *Continued*

HIP	Comp.	Date (+2000)	Filt.	$\Delta m(0.15)$ (mag)	$\Delta m(1)$ (mag)	$\theta$ ( $^\circ$ )	$\rho$ ( $''$ )	$\Delta m$ (mag)
113133	B	15.5281	I	5.5	7.3	...	...	...
115417	B	15.5255	R	4.4	6.5	180.7	0.736	2.39
115417	B	15.5255	I	4.6	6.3	180.6	0.735	1.76
116139	B	15.5281	R	4.6	5.1	...	...	...
116139	B	15.5281	I	5.6	6.9	...	...	...
116277	A	15.5255	R	4.3	4.7	...	...	...
116277	A	15.5255	I	3.9	4.5	...	...	...
117902	A	15.5282	R	5.6	8.8	...	...	...
117902	A	15.5282	I	5.8	7.6	...	...	...